PCCP

Accepted Manuscript

ROYAL SOCIETY OF CHEMISTRY

www.rsc.org/pccp

Intermolecular Interactions and Charge Transfer Transitions in Aromatic Hydrocarbon – Tetracyanoethylene Complexes

Adélia A. J. Aquino, [a,b*] Itamar Borges, Jr, [c,*] Reed Nieman,[a] Andreas Köhn,[c] and Hans Lischka[a,e*]

[a] Dep. of Chemistry and Biochemistry, Texas Tech University, Lubbock, Texas 79409-1061
[b] Institute for Soil Research, University of Natural Resources and Life Sciences Vienna, A-1190 Vienna, Austria
[c] Departamento de Química, Instituto Militar de Engenharia, Rio de Janeiro 22290-270, Brazil
[d] Institut of Theoretical Chemistry, -Universität Stuttgart, 70563 Stuttgart, Germany
[e] Institute for Theoretical Chemistry, University of Vienna, 1090 Vienna, Austria

E-mail: adelia.aquino@univie.ac.at, itamar.borges.jr@gmail.com, hans.lischka@univie.ac.at

Abstract

A comprehensive theoretical study of the electronically excited states in complexes between tetracyanoethylene (TCNE) and three aromatic electron donors, benzene, napththalene and anthracene, was performed with focus on charge transfer (CT) transitions. The results show that the algebraic diagrammatic construction method to second order (ADC(2)) provides excellent possibilities for reliable calculations of CT states. Significant improvements in the accuracy of the computed transition energies are obtained by using the scaled opposite-spin (SOS) variant of ADC(2). Solvent effects were examined on the basis of the conductor-like screening model (COSMO) which has been implemented recently into the ADC(2) method. Dielectric constant and refractive index of dichloromethane have been chosen in the COSMO calculations to compare with experimental solvatochromic effects. The computation of optimized ground state geometries and enthalpies of formation has been performed at second-order Møller-Plesset Perturbation Theory (MP2) level. By comparison with experimental data and with high-level coupled-cluster methods including explicitly correlated (F12) wave functions, the importance of the SOS approach is demonstrated for the ground state as well. In the benzene/TCNE complex, the two lowest electronic excitations are of CT character whereas in the naphthalene and anthracene TCNE complexes three low-lying CT states are observed. As expected, they are strongly stabilized by the solvent. Geometry optimization in the lowest excited state allowed the calculation of fluorescence transitions. Solvent effects lead to a zero gap between S_1 and S_0 for the anthracene/TCNE complex. Therefore, in the series of benzene/TCNE to anthracene a change from a radiative to a nonradiative decay mechanism to the ground state is to be expected.

.

Introduction

Non-covalent interactions are of crucial importance in condensed matter physics, chemistry and biology. For this reason, efficient and accurate methods for treating these types of interaction are of special interest.[1] One case of particular importance is represented by charge transfer (CT) complexes formed by the interaction of an electron donor (D) and an electron acceptor (A). These CT processes in molecular complexes constitute ubiquitous phenomena in chemistry.[2-4] They usually lead to formation of intensely colored CT complexes after absorption in the visible or UV regions.[5] In the 1950´s, Mulliken rationalized the main features of these systems through his CT theory.[6] This theory states that CT complexes have a Lewis acid – Lewis base type interaction and the bonds between the components of the complex would arise from the partial transfer of an electron from the base (electron donor D) to the acid (electron acceptor A).

CT complexes are widely used and applied in several areas of chemistry, materials science, biology and medicine.[3] In natural photosynthetic systems,[7, 8] after a CT process, "charge separation benefits from the downhill energy changes from the photoexcited state to the charge separation state".[9] In these organic systems, the energies of the CT states typically have lower energies as compared with those of the original electronic excited states of the donor. A particularly important and challenging application is found in the field of organic photovoltaics, where the population transfer to CT states at D/A boundaries plays a crucial role for the efficiency of the photovoltaic cell.[10] Most of the examples mentioned involve conjugated π systems interacting in their electronic ground or excited states.

Molecular systems bonded by delocalized π electrons and in particular π-π stacked systems have been raising a lot of interest.[11] A paradigmatic case of a photoinduced CT is given by the interaction of tetracyanethylene (TCNE) with benzene. The typical planarity of the aromatic donor systems in the examined complexes, combined with the planarity of the TCNE acceptor, can lead to quite strong non-covalent bonding interactions in the parallel stacked arrangement.[12, 13] Kuchenbecker and Jansen recently reported a comprehensive investigation of the intermolecular interaction in the benzene/TCNE complex and p-xylene/TCNE complexes in the electronic ground state using different methods including symmetry-adapted perturbation theory combined with density functional theory (DFT-SAPT) and coupled-cluster theory including non-iterative triple excitations CCSD(T).[14] In relation

to the experimental data, those authors discussed in details benzene/TCNE association energies.

In theoretical investigations of excited states in organic systems, the widely used time dependent density functional theory (TD-DFT) faces severe problems to describe correctly the stability of CT states.[15-17] Range-separated functionals[18, 19] have been developed to overcome this problem, but careful optimization of the parameter determining the separation range is necessary.[3, 20, 21] Constrained DFT optimization[22] is an alternative successfully applied to quantum mechanical/molecular dynamics (QM/MM) simulations of organic donor/acceptor interfaces.[23] Another approach, originated in the solid state community, is the many-body Green's Function Theory within the GW approximation combined with the Bethe-Salpeter equation (BSE), recently applied to study terminally substituted quarterthiophene (DCV4T)/C_{60} and aromatic donor/TCNE complexes.[24]

In contrast to DFT approaches, ab initio wave function methods do not have a general bias toward CT states. However, use of these approaches is challenging because it demands large computational resources especially in view of the usually quite extended molecular sizes of realistic molecular models. These challenges can be handled with computationally efficient methods as available, for example, in the form of the approximate coupled cluster method to second order (CC2)[25] and the closely related algebraic diagrammatic construction through second-order (ADC(2)).[26] For instance, π-conjugated oligomer systems such as methylene-bridged oligofluorenes,[27] oligo-para-phenylenes,[28] and poly(p-phenylene vinylene[29] were investigated successfully using these wave function based methods. CT states were also studied in nucleobase dimers bonded by π-π stacking interactions[30] and exciplex formation in the adenine dinucleotide [31] A crucial feature in terms of the computational efficiency of these methods is the use of the resolution of the identity (RI) approach[32, 33] that allows efficient handling of the two-electron integrals. For more information on the applicability of the ADC(2) method see also the overviews given in Refs. [34] and [35].

Grimme introduced the idea of an empirical scaling of the same and opposite spin contributions to the MP2 method in the form of spin component scaling (SCS),[36] thereby improving the accuracy of the results without increasing the computational demand. Because the SCS scaling factor was much smaller for the same spin part in comparison to the scaling factor in the opposite spin part, Head-Gordon an co-workers[37] noticed that neglecting completely the same spin part would have the same effect with only a fourth order scaling of the computational costs leading to the scaled opposite-spin (SOS) approach. This SOS ansatz

was applied also to excited states by Winter and Hättig who implemented it in the CC2 and ADC(2) methods. [38, 39] The SOS scheme has also been used successfully by Krauter et al.[40] in connection with the extended ADC(2)-x scheme. Benchmarking of SOS methods has concentrated mostly on CC2, SCS scaling and non-charge-transfer states. However, there is a recent SOS-CC2 benchmark work by the developers of the method.[39] In a test-set of 66 organic molecules for which high-resolution experimental band origins have been measured, Winter and co-workers reported that errors for SOS-CC2 are slightly smaller than for unscaled CC2, whereas unscaled ADC(2) leads to slightly larger errors than unscaled CC2.[41] In this work, for the systems examined, we show that SOS-ADC(2) results for charge-transfer states are superior to the ADC(2) values.

In our previous ADC(2) study of the poly(thieno[3,4-*b*]thiophene benzodithiophene) (PTB1)/[6,6]-phenyl-C_{61}-butyric acid methyl ester (PCBM) model systems consisting of up to 220 atoms,[42] the TCNE/benzene complex was used in preliminary investigations for comparison purposes. Now, in the present work we turn our full attention to prototypical small weak D-A bimolecular complexes consisting of aromatic donors (D = benzene, naphthalene and anthracene) and the acceptor (A) tetracyano-ethylene (TCNE).

For the accurate description of CT systems it is important to include environmental effects into the computational model. An efficient theoretical description of solvent effects is found in the polarizable continuum model (PCM).[43] Extension to excited-state solvation was developed for the TD-DFT method using linear-response and state-specific approaches.[44-48] Recently, excited-state solvation was treated within the ADC(2) method combined with the conductor-like screening model (COSMO).[49-51] Linear response as well as state-specific approaches are available in this procedure.

The TCNE molecule consists of ethylene substituted by four cyano (CN) groups and has a low-lying π^* orbital.[52] The CN group is a strongly electronegative substituent that efficiently withdraws electrons from ethylenic groups, a property that contributes to the high efficiency of TCNE as an electron acceptor in a CT complex. This charge withdrawal then enhances the electron affinity of the ethylenic group and, therefore, its Lewis π-acid strength. This property has been used in aromatic hydrocarbon-TCNE complexes leading to the appearance of CT states in low-lying electronic transitions. These excited states have been intensively investigated by means of experimental[52, 53] and theoretical methods.[3, 21, 24, 54-59] Furthermore, aromatic hydrocarbon-TCNE complexes are also considered as important benchmarks systems to assess the quality of different theoretical approaches to describe intermolecular interactions,[14] and CT transitions.[3, 21, 24, 54-59] Because these aromatic/TCNE

complexes are significantly smaller as compared to realistic donor/acceptor boundary structures (e.g., PTB1/PCBM),[42] they also provide an excellent testing ground for different theoretical methods,[3, 24, 58]in particular for the ADC(2) method used in the present work. Interest in TCNE complexes has been renewed also due to prospective applications in molecular electronic devices.[60]

The electronic spectra of aromatic hydrocarbons/TCNE complexes studied previously focused mostly on the first transition that has CT character. For that purpose, Baer and co-workers[3] employed generic and optimized range-separated hybrid functions. The aforementioned work of Baumeier *et al.* used the *GW*-BSE approximation[24] and Baruah and co-workers[58] employed a perturbative delta self-constrained DFT approach.[22] Blase and Attaccalite and collaborators [54, 55] also applied the *GW*-BSE method. Mach and co-workers used CC2, TD-DFT and CIS methods to compute the electronic excitations in TCNE complexes.[56, 57] To our knowledge, no quantum chemical calculations on solvatochromic effects for the aromatic hydrocarbons/TCNE complexes have been performed.

Earlier experimental investigations of the aromatic-TCNE complexes examined in this work concentrated on thermodynamic properties of the vapor and liquid phases.[52, 53, 61] Recently, Chiu and co-workers did a very thorough study of the complicated CT-state photodynamics of benzene/TCNE including fluorescence measurements.[62] For the other complexes, fluorescence measurements were not found in the literature.

The purpose of our work is to examine in detail three TCNE complexes with benzene, naphthalene and anthracene, respectively, starting with ground state properties but then concentrating on the balanced treatment of a multitude of excited states with emphasis on the low-lying (i.e., below 5.0 eV) transitions of the TCNE complexes because of their CT character and availability of experimental data. Geometry optimizations in the S_1 state relevant for the analysis of fluorescence spectra as well as solvent effects will be discussed. The approaches used in this work are dedicated to the ADC(2) method and its scaled SOS variant, SOS-ADC(2),[39] which allow a wide-ranged and accurate description of energetic and structural aspects of CT complexes. The aforementioned combination of ADC(2) and COSMO is used to discuss the solvent effects on electronic excitations.

Computational Details

Three distinct systems, each one involving a combination of an aromatic donor – benzene, naphthalene and anthracene (in two orientations), forming a stacked complex with the acceptor TCNE (Scheme 1), were investigated. The geometry optimizations of the

benzene/TCNE, naphthalene/TCNE and anthracene/TCNE ground state structures were carried out using the standard MP2[63] and the SOS modification of MP2[37] using in both cases the resolution of the identity (RI) approach.[33, 64] For excited state calculations the ADC(2) [26, 35] and SOS-ADC(2)[38, 39] approaches were chosen as implemented in the Turbomole[38] program suite.

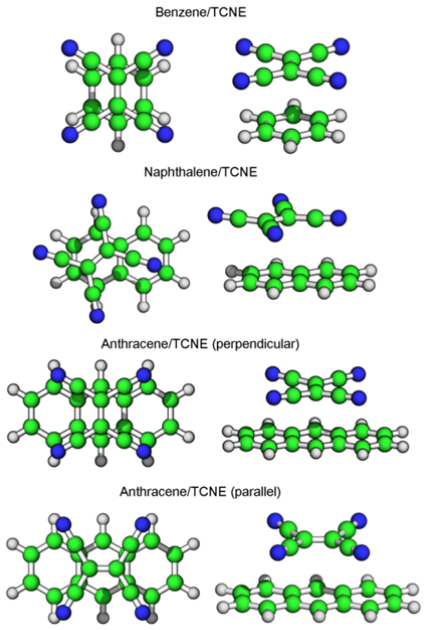

Scheme 1. Top (left) and side (right) views of the benzene/TCNE, naphthalene/TCNE and anthracene/TCNE complexes.

In the case of the MP2/COSMO ground state geometry optimizations, we used the energy-consistent formalism via the perturbation theory "energy-only" (PTE) scheme described for PCM in Ref.[65]. Single point calculations were additionally performed for the benzene/TCNE ground-state complex using the coupled cluster with singles and doubles (CCSD) and with non-iterative triples (CCSD(T)) methods,[66] and the explicitly correlated CCSD(F12*)[67] approaches.

Calculation of the standard enthalpies ΔH_{298} of formation assumes an ideal gas and no coupling between internal degrees of freedom. The standard approximations, namely, rigid rotor for rotation, the quantum harmonic oscillator for the vibrational modes and a constant value for the electronic contribution are used.[68]

Excited states were computed using the RI-ADC(2) and RI-SOS-ADC(2) methods. Excited-state geometry optimizations were normally performed for the first excited state, which always had CT character in this investigation. For benzene/TCNE, the geometry of the second excited state was also optimized because it was close in energy to the first one and was also a CT state. Fluorescence transition energies were computed as the vertical de-excitation at the optimized geometry of the lowest excited state. Adiabatic, i.e., minimum to minimum excitation energies, were obtained also.

The calculations were carried out for the isolated complexes and including the solvent effects though the COSMO approach.[50] For ADC(2)/COSMO calculations of the excited states, the recently developed state-specific approach was used.[51] The parameters for the dielectric constant ε and the refractive index n (ε = 10.7, n = 1.42[69]) were chosen to represent dichloromethane (CH_2Cl_2), a solvent of medium polarity. For simplicity, the COSMO results are indicated further on with the label dichloromethane. For the excited states, ADC(2)/COSMO calculations were performed in two different scenarios. In the first, the solvation of the excited states was obtained using the ground state density as reference and taking into account by means of the state-specific approach only the fast electronic relaxation. In the second scenario, the equilibrated solvation of the selected excited state was considered.

The triple zeta basis sets of Dunning, with (aug-cc-pVTZ) and without diffuse (cc-pVTZ) functions,[70, 71] were used. After analyzing test calculations, for the naphthalene/TCNE and anthracene/TCNE complexes, a mixed basis set with cc-pVTZ applied to the carbon and nitrogen atoms and cc-pVDZ for the hydrogen atoms was constructed and denoted cc-pVTZ'. For the F12 calculations, an approach which includes the inter-electronic distance r_{12} explicitly in the wave function, the cc-pVDZ-F12 basis set[72] was used.[73] These basis sets were selected because they provided sufficient accuracy without being computationally too demanding.

The intermolecular perpendicular distance between benzene and TCNE, the intramolecular carbon-carbon distances of the aromatic systems and TCNE and the carbon-nitrogen distances of TCNE were examined. Basis set superposition error (BSSE) was included using the counterpoise (CP) correction[74] for the benzene/TCNE complex.

The quantification of the charge transferred for a given electronic transition was obtained using a recently developed CT descriptor q(CT).[75] This descriptor is based on the analysis of the transition density matrix in terms of constituent fragments. If q(CT) equals 1e, e being the electronic charge, a complete charge transfer of one electron has occurred while

for q(CT) = 0 the transition is a locally excited state. For the electronic ground state, the CT value was calculated using the natural population analysis (NPA).[68, 76]

Bond length alternation (BLA) values[77] were obtained from bond length differences to characterize geometry changes due to electronic excitations. For the complexes in this work, the BLA values were computed for the aromatic systems according to the following expressions:

Benzene:

$$BLA_{benzene} = 1/2(b_2 + b_5) - 1/4(b_1 + b_3 + b_4 + b_6) \quad (1)$$

Naphthalene:

$$BLA_{naphtalene} = 1/4(b_1 + b_3 + b_6 + b_8) - 1/7(b_2 + b_4 + b_5 + b_7 + b_9 + b_{10} + b_{11}) \quad (2)$$

Anthracene:

$$BLA_{anthracene} = 1/4(b_1 + b_3 + b_8 + b_{10}) -$$
$$-1/12(b_2 + b_4 + b_5 + b_6 + b_7 + b_9 + b_{11} + b_{12} + b_{13} + b_{14} + b_{15} + b_{16}) \quad (3)$$

The bond numbers b_i are defined in Scheme 2.

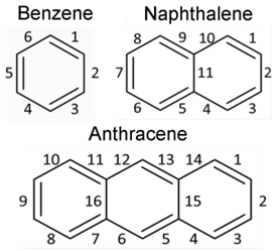

Scheme 2. Bond numbering scheme for the aromatic compounds used in the context of the bond length alternation analysis (BLA). See the text for details.

The Turbomole program[78] version 6.4 was used for the gas phase calculations. The COSMO calculations were performed with a TURBOMOLE development version.

Results and Discussion

The complexes between TCNE and the aromatic compounds were built as sandwich structures with the two molecules lying parallel to each other. This arrangement,

inferred from independent experiments made by Merrifield and Phillips[52] and Hanazaki,[53] favors maximum overlap between the π-molecular orbitals of the two molecules and thus the appearance of CT bands. These stacked-type conformations were also used in previous theoretical investigations.[3, 54-57]

The TCNE molecule is located over the middle portion of the aromatic ring. In Scheme 1 the four investigated structures, including the two arrangements of the anthracene/TCNE complex, are displayed. The Cartesian coordinates of the four complexes are given in the Supporting Information.

For benzene/TCNE, the benzene molecule was set parallel to TCNE and the C=C bond of TCNE was oriented along two benzene CH bonds. For the naphthalene/TCNE complex, geometry optimizations converged to TCNE dislocated with respect to the center of the molecule and twisted by about 45 degrees with respect to the vertical axis. This arrangement resulted in the naphthalene complex having C_1 symmetry as compared to the C_{2V} symmetry found in the benzene and anthracene complexes. For the anthracene/TCNE complex, two possible orientations were considered: the perpendicular one has the TCNE C=C bond aligned with the HCCH axis over the central anthracene ring while in the parallel geometry, the TCNE C=C bond was aligned along the direction of the three benzene rings, i.e., the TCNE molecule was rotated by 90º (see Scheme 1). Benzene was arranged in the xy plane and the CC bond of TCNE oriented along the x-axis. In case of the perpendicular complex, anthracene was located in the xy plane and the CC bond of TCNE oriented along the x axis. For the parallel complex, the TCNE molecule was rotated by 90º.

We also examined another configuration of the benzene/TCNE complex with TCNE rotated by 90º around the C_6 axis of benzene and having its carbon atoms located over the carbon-carbon bonds of the benzene molecule instead of over its carbon atoms. The converged structure of C_{2V} also corresponded to a local minimum. This structure was slightly less stable by +0.032 kcal/mol and we chose to proceed only with the more stable one.

The internal structure of the molecules in the ground state complexes is only slightly perturbed upon complex formation thus confirming previous results.[3] Table 1 collects selected bond distances of the four optimized arrangements computed with MP2 and SOS-MP2. Effects of solvation in dichloromethane of the complexes and gas-phase charge transfer q(CT) values are shown also. For the benzene/TCNE complex, results with different basis sets are also reported. Inspection of the data shows only small variations in the selected bond distances with basis set size. A similar observation can be made for counter-poise corrections and dichloromethane solvation. A different situation is found for the intermolecular

separation distances using SOS-MP2: the separation distances in the four complexes increase significantly in the range of 0.2 Å - 0.25 Å.

Overall, the MP2 separation distances both in gas-phase and in dichloromethane are about 3.0 Å, the exception being the anthracene/TCNE(perp.) complex with a value of ~0.2 Å smaller. The separation distances between the aromatic donor and the TCNE acceptor, both in gas-phase and in dichloromethane, show a decreasing order using the MP2/cc-pVTZ' (MP2/cc-pVTZ for the benzene complex) and SOS-MP2 approaches: benzene/TCNE > naphthalene/TCNE > anthracene/TCNE (perp.). The bonding in the anthracene/TCNE (parallel) complex is weaker as compared to the perpendicular complex and displays also an increase in the separation distance.

The MP2 wave function can treat accurately long range-interactions, dispersion, polarization, but it overestimates the π–π interactions in π–stacked systems.[79] These effects are certainly important for the TCNE complexes, especially the latter. Because the SOS flavor of MP2 improves the accuracy of the results over the standard MP2,[37] the SOS-MP2 geometry parameters reported in Table 1 should be superior to MP2 ones. This fact was confirmed in the computed association energies, which get closer to experiment with SOS-MP2 (see below).

The amount of CT q(CT) given in Table 1 indicates that the ground state of the complexes does not possess CT character, the exception being anthracene/TCNE (perp.) having the non-negligible value of 0.22e. In this case, we could argue that an almost perfect bond alignment of both molecules in this configuration in the ground state (see Scheme 1, top view), in comparison with the other systems, greatly favors the interaction between their π systems, which could explain the appearance of some amount of CT in the ground state.

Our computed CT q(CT) value of 0.047e for the benzene/TCNE complex can be compared with the value of 0.075e deduced by Kubiak and co-workers from infrared spectra.[60]

Table 2 shows the calculated association (i.e. interaction) energies ΔE_{ass} and standard enthalpies ΔH_{298}. All the association energies and standard enthalpies are negative; thereby formation of the TCNE complexes is an exothermic process. For benzene/TCNE, extension of the basis set by diffuse functions can affect the ΔE_{ass} values leading to differences of about 10%. The difference between ΔE_{ass} and ΔH_{298} is about 10% and brings the computed results closer to experiment. Nevertheless, the interaction energies calculated at the MP2 level are, as expected, still much too strong when compared with the available experimental values. The

SOS-MP2 approach, however, considerably improves the agreement with experiment by greatly decreasing the computed interaction energies. Even without inclusion of zero-point energy effects, the discrepancies between the SOS-MP2 results and the available measurements for benzene/TCNE and naphthalene/TCNE are significantly reduced in comparison with the MP2 result. An even larger reduction is observed for the two anthracene complexes with respect to the MP2 values. As a result, by using the SOS-MP2 approach in Table 2 a pronounced improvement of the association energies compared to experiment is seen, which is reflected also in larger separation distances (see Table 1).

The coupled-cluster method is currently the most accurate wave function method to describe systems involving non-covalent interaction including dispersion.[79, 80] For this reason, we tested different types of coupled-cluster approaches (Table 2). In particular, for the benzene/TCNE complex ΔE_{ass} was also computed using the CCSD(F12*)(T)/cc-pVDZ-F12 method, that allows highly accurate calculations of intermolecular interaction energies.[13, 80, 81] The F12 method was also found to be less susceptible to BSSE problems.[73] The ΔH_{298} value of -6.95 kcal/mol computed with this method is in excellent agreement with the experimental value of -6.6 kcal/mol (Table 2). The CCSD(T)/cc-pVTZ interaction energy comes also close to the CCSD(F12*)(T)/cc-pVDZ-F12 benchmark result whereas the interaction computed at CCSD/cc-pVTZ level appears to be too weak. However, all of these interaction energies constitute significant progress as compared to the strongly over-binding MP2 method. It is especially gratifying that the SOS-MP2/cc-pVTZ approach provides a very satisfactory result since because of its computational efficiency it allows investigations of significantly larger systems than the benzene/TCNE complex.

The SOS-MP2 benzene – TCNE distance is 3.22 Å (Table 1), equal to the DFT-SAPT/CBS(TQ) and CCSD(T)-F12b/ cc-pVDZ-F12 most accurate distances of Kuchenbecker and Jansen.[14] Their ΔE_{ass} values obtained with these two methods are respectively -8.38 kcal/mol and -8.47 kcal/mol, in good agreement with our values of -8.99 kcal/mol (SOS-MP2/cc-VTZ), -8.82 kcal/mol (CCSD(T)/cc-pvTZ) and -8.56 kcal/mol (CCSD(F12*)(T)) in Table 2. Concerning ΔH_{298} values, Kuchenbecker and Jansen report -7.16 kcal/mol using BLYP-D/TZVPP, which should be compared with our CCSD(F12*)(T) value of -6.95 kcal/mol using the MP2/cc-pVTZ geometry (Table 2). The experimental value is -6.6 ± 03 kcal/mol measured in the range of temperatures of about 373 – 423 K.[53, 61] Therefore, the results of this study and Kuchenbecker and Jansen´s value agree quite well

with the experiment, although those authors argue for the importance of new experimental measurements.

Vertical excitation energies ΔE_{exc}, oscillator strengths (f) and charge transfer values q(CT) of the lowest excited states are presented in Table 3 (benzene/TCNE), Table 4 (naphthalene/TCNE), Table 5 (anthracene/TCNE perpendicular) and Table 6 (anthracene/TCNE parallel). The Tables S4-S7 collect excitation energies of eight electronic states for each complex.

The lowest excited states of the four molecular complexes have a strong CT character with almost a full charge transferred to the TCNE acceptor. While for benzene/TCNE only the two almost degenerate (because of the double degenerate HOMOs in isolated benzene) lowest excited states are of CT type (Table 3 and S4), for naphthalene/TCNE (Table 4 and S5) and both anthracene/TCNE complexes (Table 5, Table 6, Table S6 and S7), the three lowest states possess CT character. When solvated in dichloromethane, the CT character of the states is maintained, including the magnitude of the charge transferred. Once any one of the complexes is electronically excited, a higher bright locally excited state can decay into one of the lower CT excited states. A similar picture was also found for the PTB1/C_{60} composite.[42] This feature, namely the decay of a bright state into a lower CT excited state, is a crucial property for the functioning of an important technical application of donor-acceptor complexes – the organic solar cells. For these systems, the CT state is then followed by charge separation ultimately leading to formation of an electric current.[10]

Table 3 displays the vertical excitation energies of the benzene/TCNE complex computed under several conditions such as different basis sets, ground state geometries and the ADC(2) method with and without the SOS approach. Inspection of the gas phase data shows that extension of the cc-pVTZ basis with an augmented basis changes the excitation energies only to a small extent by ~0.02 eV. Increasing the intermolecular distance of the complex by using the SOS-MP2 geometry has a slightly larger effect of ~0.05 eV. A significantly larger change is found when the spectra are computed using SOS-ADC(2). In this case, the excitation energies increase by ~0.5 eV as compared to the ADC(2) value. Therefore, using for the benzene/TCNE complex the SOS-ADC(2) method instead of ADC(2) improves the agreement with the experimental transition energy from an underestimation by -0.31 eV to a smaller overestimation of +0.18 eV.

It should be mentioned that more CT states at higher excitation energies were found for the complexes with the larger aromatic compounds. In the case of naphthalene/TCNE, the

first two states above 5 eV (8^1A and 9^1A) also have CT character (Table S5). A similar situation is observed for the anthracene/TCNE complexes (Tables S6 and S7). The appearance of higher CT states in these complexes stems from the higher availability of π electrons on the larger naphthalene and anthracene donors in contrast with the smaller benzene donor.

For the naphthalene/TCNE complex (Table 4), the lowest three states have CT character except in one case: the SOS-ADC(2) 4^1A state in the gas phase corresponds to a local excitation. The MP2 geometry and ADC(2) excitation energy lead to gas phase results with too low excitation energies (-0.55 eV for the first absorption band). This discrepancy is significantly reduced in absolute value to 0.19 eV by using the corresponding SOS version of the MP2 and ADC(2) wave functions.

For the anthracene/TCNE complex, there are no experimental gas-phase measurements. Therefore, in this case we concentrate on the differences between the standard ADC(2) and SOS-ADC(2) results (Table 5 and Table **6**). As for the complexes containing benzene and naphtalene, the SOS-ADC(2) excitation energies are larger in comparison with the ADC(2) values. This effect is not as large for the perpendicular configuration as compared to the parallel one. Furthermore, the electronic excitations of the perpendicular and parallel complexes show a different ordering. Whereas in the perpendicular case (Table 5) the bright 2^1A_1 is the lowest singlet excited state and the dark 1^1A_2 state is the second one. The situation is reversed for the parallel anthracene-TCNE complex (Table 6): now the dark 1^1A_2 state has lowest energy. This difference has important implications for the comparison to the experimental spectrum in dichloromethane to be discussed below.

Electron density difference plots between the electronic ground state and the lowest excited state having CT character for three complexes are displayed in Figure 1 to Figure 4. The depletion of the aromatic π system and the filling of the π* system of TCNE can be nicely followed in all figures. The electron-withdrawing ability of the nitrogen atoms in TCNE is also evident in all cases. An interesting difference between the density difference plots for the almost degenerate dark 1^1A_2 (Figure 1) and bright 2^1A_1 (Figure 2) states of the benzene/TCNE can be noted. In the first case, the depletion of electron density occurs in benzene along the two benzene CC bonds parallel to the CC bond in TCNE whereas in the second case the depletion occurs in the complementary part of the benzene molecule. These features will be discussed below in the framework of the BLA changes occurring in the excited state geometries.

When not stated differently, solvent effects were computed within COSMO using the equilibrated ground state solvent structure and a non-equilibrium approach for the vertical electronic excitation based on the fast electronic relaxation described by the refractive index *n*.[82] Alternatively, COSMO calculations were performed with solvent charge equilibration for the excited state.

For the benzene/TCNE complex, the computed solvent shifts (Table 3) lie in a range about 0.55 – 0.65 eV quite independently of the geometry and the fact whether the SOS-ADC(2) method was used or not. The experimental shift is 0.365 eV, a bit smaller compared with the computed range. The agreement between the most reliable result of this work (SOS-MP2 geometry and SOS-ADC(2)) for the symmetry allowed 2^1A_1 state and the experimental excitation energy is very good; both energies agree within the range of 0.1 eV. For a methodological comparison, the excitation energies for solvent equilibration in the field of the electron distributions of the 1^1A_2 and 2^1A_1 states were also calculated. This approach will be used for the discussion of solvatochromic shifts of the fluorescence transitions given later in the text. The resulting additional solvent shifts deriving from the specific solvation of the excited states as compared to the original ground state solvation are 0.484 eV ($^1A_2$) and 0.453 eV (2^1A_1), respectively.

The SOS-ADC(2) calculations for the naphthalene/TCNE complex solvated in dichloromethane using the SOS-MP2 geometry show excellent agreement with experimental excitation energies for the CT bands I and II (Table 4).

In the solvated perpendicular anthracene/TCNE, the excitation energy of the 2^1A_1 state (Table 5) agrees very well with the experimental band I once again using the combination of a SOS-MP2 geometry and the SOS-ADC(2) method. The solvation energy contribution to the electronic excitation is within about −0.5 eV for all states, similar to the other examined complexes. The ADC(2) (non SOS) solvent shifts are at most 0.05 eV smaller. The calculated excitation energy of the S_2 (1^1A_2) state would agree well with the measured CT band II energy, but it is symmetry forbidden; on the other hand, intensity can be gained due to vibronic effects.[83] The next transition (1^1B_2) would be 0.55 eV too high in comparison with the CT band II when using the SOS-ADC(2) method.

The excitation energies computed for the parallel anthracene/TCNE complex (Table 6) do not agree well with the experimental band system (Table 5). In this case, the bright 2^1A_1 state is located at 2.79 eV corresponding to the CT band II of perpendicular anthracene/TCNE complex and there is no absorption intensity computed for the region

around 1.7 eV where the intense experimental CT band I of the perpendicular complex lies (see Table 5). This mismatch is in line with the lesser stability of the parallel complex in the ground state (Table 2) which both indicate that the perpendicular arrangement is found in the experiment.

SOS-ADC(2) geometry optimizations were done for the lowest excited states of the isolated complexes. Selected geometry parameters are collected in Table 7. Comparison of the aromatic – TCNE separation distances of the ground state (Table 1) and the excited state (Table 7) results in the following picture when looking at increasing size of the aromatic donor. For the benzene/TCNE (1^1A_2) complex, a marginal increase of 0.01 Å (1^1A_2) and decrease of 0.02 Å (2^1A_1) is observed with respect to the ground state value (SOS-MP2 geometry and SOS-ADC(2)). In the case of naphthalene/TCNE, the intermolecular distances increases by 0.23 Å, and for the perpendicular anthracene/TCNE the increase amounts to 0.37 Å. Nevertheless, at the relaxed geometries the excited states maintain, as expected, the strong charge transfer character – see the corresponding *q*(CT) values. The CC and CN distances in TCNE and the charge transfer values *q*(CT) are quite insensitive to the relaxation of the excited state geometries.

The analysis of the BLA values (Table 7), obtained according to equations (1)-(3), highlights the geometry changes in the behavior of the aromatic systems. A positive BLA value for the benzene complex in the 1^1A_2 state reflects a quinoidal stretching along the bonds b_2 and b_5 that are parallel to the TCNE CC bond (Scheme 1). The other benzene bonds are slightly shortened. This stretching also agrees nicely with the preferential region of electron density depletion in the benzene subsystem (Figure 1). On the other hand, for the almost degenerate 2^1A_1 state, the positive BLA value in benzene/TCNE indicates a shortening of these CC bonds and a stretching of the others. This alternative bond stretching in benzene correlates nicely with the different regions of charge depletion for the two states (Figure 1 and 2). In the naphtalene complex, the bonds b_1, b_3, b_6 and b_8 are stretched which leads to a change in the BLA from originally -0.047 Å for the ground state to the positive value of 0.002 Å in the first excited state. The elongation of the four mentioned bonds at the ends of naphtalene agrees well with the localized depletion of electron density as shown in the density difference plot of Figure 3. In the perpendicular anthracene complex, where the bonds b_1, b_3, b_8 and b_{10} are stretched, a similar situation is observed. This leads to a change in the BLA from originally -0.052 Å for the ground state to a less negative value of -0.017 Å in the first excited state. These geometrical changes also agree also with the localized depletion of electron density as shown in the density difference plot of Figure 4.

Table 8 collects the adiabatic (minimum to minimum) absorption and the vertical fluorescence energies for three complexes. The corresponding vertical absorption energies can be found in Table 3-Table 5. In the gas phase, the structural relaxation leads to an energetic stabilization in the excited state of 0.4-0.5 eV in relation to the vertical excitation (SOS-ADC(2)). The vertical fluorescence transition to the ground state reduces the S_0/S_1 gap by an additional amount of ~0.5 eV. The COSMO results in Table 8 were obtained for the minimum-to-minimum transition with equilibration of the solvation shell for the ground state and the excited state separately. In case of the fluorescence process, the solvent equilibration was performed for the respective excited state. For the transition to the ground state, only the fast electronic solvent relaxation was included in analogy to the reverse process of the computation of the absorption spectra. The solvent effect amounts to ~1.3 eV in the case of the fluorescence transition in the benzene complex. The effect on the minimum-to-minimum transition is lower (0.8 eV). Rather small solvent shifts are observed for the other complexes. The gap for the fluorescence transition decreases from 1.38 eV in benzene/TCNE to 0.77 eV in naphthalene/TCNE. Going to anthracene/TCNE in the next step leads to a vanishing gap (the transition energy is actually -0.13 eV) which means that a conical intersection exists. It should be noted that ADC(2) is based on a single Hartree-Fock determinant and is not well suited to describe conical intersections with the ground state. Nevertheless, it can be expected that the qualitative features of the intersection can be described quite at this computational level as has been shown in investigations of the conical intersections for adenine using ADC(2) [84] and the related CC2 method.[85] Multireference calculations are certainly required to obtain a more complete picture of the photodeactivation processes of these types of CT complexes. Nonetheless, the present calculations indicate a change in the photodeactivation mechanism from a radiative fluorescence to ultrafast nonradiative processes in polar solution.

To our knowledge, fluorescence measurements are only available for the benzene/TCNE complex. In a recent work, the steady state fluorescence spectrum of benzene/TCNE solvated in dichloromethane was measured with a maximum at ~ 1.65 eV. The above-mentioned computed value of 1.38 eV in solution (Table 8) agrees very well with this experimental value.[62] The geometry optimizations on the excited states of the benzene/TCNE complex where performed using C_{2v} symmetry as for the ground state. TDDFT geometry optimization of the first excited state reported in Ref. [62] show an off-centered position of TCNE with respect to benzene indicating large amplitude intermolecular motions. Preliminary ADC(2) calculations on the S_1 state seem to confirm the TDDFT

findings. However, more detailed ADC(2) calculations have not been performed since they go beyond the scope of the present work.

Conclusions

In this work, we carried out a detailed investigation of three prototypical complexes containing an aromatic donor and a TCNE acceptor. The aromatic molecules were benzene, naphthalene and anthracene. These complexes are bonded by π–π stacked interactions and their first excited states are of charge transfer (CT) type. The goal of our investigations was the accurate quantum chemical description of these two challenging problems using computational methods that can be applied to significantly larger complexes as well.

The scaled opposite spin (SOS) type wave functions were explored in this work in conjunction with the MP2 and ADC(2) methods for ground and excited states, respectively. The SOS-ADC(2) approach was used also to optimize excited state geometries and to compute fluorescence energies. The environmental effects were described by means of a state-specific approach available in a recently developed version of the COSMO method for ADC(2).

For the bonding in the benzene-TCNE complex, good agreement was found between our ground state association energies and internuclear SOS-MP2 distances with available experimental data and previous high-level calculations. Up to eight electronically excited states were computed which included CT and locally excited states. In comparison with experimental transition energies, ADC(2) underestimated the CT transitions by several tenths of an eV whereas SOS-ADC(2) gave significantly improved results. Furthermore, the computed solvent effects based on COSMO calculations resulted in very satisfactory solvatochromic shifts when compared to experimental data. Optimization of the lowest excited state structures aids the understanding of fluorescence processes. Again, the computed fluorescence transition energy compares well with the available experimental fluorescence maximum for the benzene/TCNE complex. To our knowledge, experimental fluorescence data for the naphthalene and anthracene are not available. Solvent effects lead to a zero gap between S_1 and S_0 for the anthracene/TCNE complex. Therefore, from the sequence of diminishing S_1/S_0 gaps a change from a radiative to an ultrafast nonradiative photodeactivation mechanism is inferred when going from the benzene- to the anthracene/TCNE complex in a polar solution.

To summarize, a major conclusion of this work is the potential of the SOS variant of MP2 and ADC(2) to give more accurate results of interaction energies and excited state properties for the π–π stacked CT complexes examined in this work. By comparison with higher level CCSD(T) and CCSD(F12*)(T) calculations, we have shown that the SOS-MP2 method is an accurate approach to describe π-stacked interactions with molecules containing strongly polar bonds. Most importantly, the SOS-ADC(2) method provides accurate results for transition energies, oscillator strengths and CT values for a broad range of electronically excited states including geometry optimizations in the excited state. For describing environmental effects in excited states, the COSMO approach gave good results for the discussion of solvatochromic effects of absorption and emission processes. This work is also intended to provide the basis of photodynamical simulations of internal conversion processes from locally excited π-π* states to the CT states and eventually also to the ground state.

Acknowledgments

IB thank the Brazilian Agencies CNPq, Faperj and Capes for support of this work. HL and IB acknowledge support from Capes in the framework of the Brazilian Science without Borders Program. HL is "Bolsista CAPES/Brasil". This material is based upon work supported by the National Science Foundation under Project No. CHE-1213263 and by the Austrian Science Fund within the framework of the Special Research Program F41. Computer time at the Vienna Scientific Cluster (Project nos. 70019 and 70376) is gratefully acknowledged. Support was also provided by the Robert A. Welch Foundation under Grant No. D-0005 and by the Center for Integrated Nanotechnologies (Project No. C2013A0070), an Office of Science User Facility operated for the U.S. Department of Energy Office of Science by Los Alamos National Laboratory (Contract DE-AC52-06NA25396) and Sandia National Laboratories (Contract DE-AC04-94AL85000).

Supporting Material. Interaction energies of the four complexes as well as vertical excitation energies of up to eight states are reported. The SOS-MP2 Cartesian coordinates of the optimized geometries of the four complexes are also given.

Table 1. Selected bond distances (Å) for the benzene/TCNE complex, charge transfer *q*(CT) in units of *e* from the aromatic compound to TCNE in the electronic ground state using the MP2 method with different basis sets and bond length alternation (BLA) values. The results refer to the gas phase and the standard MP2 method without CP correction unless indicated otherwise.

Basis set	TCNE/Aromat.[a]	CC(aromat.)[b]	BLA[c,d]	CC(TCNE)	CN	*q*(CT)
			Benzene/TCNE			
cc-pVTZ	3.015	1.396	-0.004	1.413	1.176	0.047
SOS/cc-pVTZ	3.224	1.397	-0.002	1.424	1.169	-
aug-cc-pVTZ	2.971	1.396	-0.003	1.413	1.176	-
with CP corr.						
cc-pVTZ	3.086	1.395	-0.002	1.413	1.176	-
aug-cc-pVTZ	3.036	1.396	-0.003	1.411	1.176	-
Dichloromethane						
cc-pVTZ	2.992	1.397	-0.004	1.412	1.175	-
			Naphtalene/TCNE			
cc-pVTZ’	2.971	1.402	-0.039	1.413	1.177	0.055
SOS/cc-pVTZ’	3.192	1.405	-0.047	1.420	1.169	-
Dichloromethane						
cc-pVTZ’	2.932	1.403	-0.039	1.413	1.176	-
			Anthracene/TCNE (perpendicular)			
cc-pVTZ’	2.828	1.405	-0.034	1.403	1.179	0.226
SOS/cc-pVTZ’	3.091	1.408	-0.052	1.420	1.170	-
Dichloromethane						
cc-pVTZ’	2.772	1.406	-0.032	1.404	1.179	-
			Anthracene/TCNE (parallel)			
cc-pVTZ’	3.024	1.406	-0.045	1.413	1.177	0.032
SOS/cc-pVTZ’	3.233	1.409	-0.056	1.421	1.169	-
Dichloromethane						
cc-pVTZ’	3.008	1.406	-0.046	1.413	1.176	-

[a] perpendicular distance between TCNE and the aromatic counterpart.
[b] average CC distance in the aromatic system.
[c] See Eqs. (1-3).
[d] Monomer values, SOS-MP2/cc-pVTZ: benzene 0.0 Å, naphthalene -0.047 Å, anthracene -0.055 Å

Table 2. Association energies ΔE_{ass} and standard enthalpies ΔH_{298} in kcal/mol for the TCNE complexes computed with selected basis sets in comparison to experimental data.

Basis set	ΔE_{ass}	ΔH_{298}
Benzene/TCNE		
MP2/cc-pVTZ	-14.10	-12.49
MP2/aug-cc-pVTZ	-16.09	
MP2/cc-pVTZ/CP	-11.73	
MP2/aug-cc-pVTZ/CP	-13.42	
SOS-MP2/cc-pVTZ	-8.99	
CCSD/cc-pVTZ[a]	-6.38	
CCSD(T)/cc-pVTZ[a]	-8.82	
CCSD(F12*)(T)/cc-pVDZ-F12 [a]	-8.56	-6.95[b]
exp. (gas)[c]		-6.6 ± 0.3.
naphthalene/TCNE		
MP2/cc-pVTZ'	-18.15	-16.49
SOS-MP2/ cc-pVTZ'	-11.10	-9.44[b]
exp. (gas)[c]		-7.67 ± 0.09
anthracene/TCNE(perp.)		
MP2/cc-pVTZ'	-25.84	-24.24
SOS-MP2/cc-pVTZ'	-13.47	-11.87[b]
anthracene/TCNE (parallel)		
cc-pVTZ'	-19.61	-17.94
SOS-MP2/cc-pVTZ'	-12.04	-10.37[b]

[a] MP2/cc-pVTZ geometry.
[b] Value estimated from cc-pVTZ or cc-pVTZ' results.
[c] Ref. [53]

Table 3. Vertical excitation energies ΔE_{exc} for the two lowest CT states of the benzene/TCNE complex using the ADC(2) and SOS-ADC(2) methods, respectively, and different basis sets. Charge transfer [q(CT)] in units of e and oscillator strengths are also shown.

Geometry	State	ΔE_{exc}(eV)[a]		Solv. Shift (eV)		f[b]	q(CT)[b]
		ADC(2)	SOS-ADC(2)	ADC(2)	SOS-ADC(2)		
Gas phase							
MP2/cc-pVTZ[b]	1^1A_2	3.229		-	-	0.0	0.95
	2^1A_1	3.283		-	-	0.086	0.93
MP2/aug-cc-pVTZ	1^1A_2	3.208		-	-	0.0	0.94
	2^1A_1	3.265		-	-	0.093	0.92
SOS-MP2/ cc-pVTZ	1^1A_2	3.280	3.754[c]	-	-	0.0	0.97[c]
	2^1A_1	3.318	3.772[c]	-	-	0.058[c]	0.96[c]
Exp.[d]		3.589		-	-	0.019	-
Dichloromethane							
gs-solv MP2/cc-pVTZ[e,f]	1^1A_2	2.678		0.551		0.0	0.95
	2^1A_1	2.726		0.557		0.101	0.93
SOS-MP2/ cc-pVTZ[f]	1^1A_2	2.707	3.176	0.573	0.578	0.000[c]	0.97[c]
	2^1A_1	2.730	3.126	0.588	0.646	0.080[c]	0.96[c]
Exp.[g]			3.224		0.365	-	-
exc-solv							
SOS-MP2/ cc-pVTZ[f]	1^1A_2		2.692[h]		1.062	0.0	0.97[c]
	2^1A_1		2.673[h]		1.099	0.080	0.96[c]

[a] Same basis set used as for geometry optimization.
[b] ADC(2) results unless specified differently.
[c] SOS-ADC(2).
[d] Ref.[86]
[e] cc-pVTZ results from Table S11 in our previous work.[42]
[f] Gas phase geometry.
[g] Ref.[52]
[h] Ground state energy computed with ground-state equilibrated solvent.

Table 4. Vertical excitation energies ΔE_{exc} for the three lowest CT states of the naphthalene /TCNE complex using the ADC(2) and SOS-ADC(2) methods, respectively, and the cc-pVTZ' basis. Charge transfer [q(CT)] in units of e and oscillator strengths are also shown.

Geometry	State	ΔE_{exc} (eV)		Solv. Shift (eV)		f[a]	q(CT)[a]
		ADC(2)	SOS-ADC(2)	ADC(2)	SOS-ADC(2)		
Gas phase							
MP2	2^1A	2.149		-	-	0.008	0.96
	3^1A	2.958		-	-	0.072	0.93
	4^1A	4.077		-	-	0.028	0.90
SOS-MP2	2^1A	2.209	2.793	-	-	0.007[b]	0.979[b]
	3^1A	2.954	3.412	-	-	0.053[b]	0.964[b]
	4^1A	4.105	4.352	-	-	0.001[b]	0.040[b]
Exp.[c]	CT Band I		2.600	-	-	0.010	-
Exp.[c]	CT Band II		3.230	-	-	0.014	-
Dichloromethane							
MP2[d]	2^1A	1.660		0.489		0.010	0.95
	3^1A	2.493		0.456		0.082	0.93
	4^1A	3.626		0.451		0.032	0.92
SOS-MP2[d]	2^1A	1.710	2.292	0.499	0.501	0.009[b]	0.97[b]
	3^1A	2.470	2.919	0.484	0.593	0.060[b]	0.96[b]
	4^1A	3.630	4.207	0.475	-0.145	0.024[b]	0.96[b]
Exp.[e]	CT Band I		2.257		0.343	-	-
	CT Band II		2.901		0.329	-	-

[a] ADC(2) results unless specified differently.
[b] SOS-ADC(2) results.
[c] Ref.[53]
[d] Gas phase geometry.
[e] Ref.[52]

Table 5. Vertical excitation energies ΔE_{exc} for the three lowest CT states of the anthracene/TCNE perpendicular complex using the ADC(2) and SOS-ADC(2) methods, respectively, and the cc-pVTZ' basis. Charge transfer [q(CT)] in units of e and oscillator strengths are also shown.

Geometry	State	ΔE_{exc} (eV)		Solv. Shift (eV)		f[a]	q(CT)[a]
Gas phase		ADC(2)	SOS-ADC(2)	ADC(2)	SOS-ADC(2)		
MP2	2^1A_1	2.113		-	-	0.180	0.79
	1^1A_2	3.028		-	-	0.0	0.86
	1^1B_2	3.200		-	-	0.043	0.84
SOS-MP2	2^1A_1	1.783	2.223	-	-	0.131[b]	0.902[b]
	1^1A_2	2.873	3.243	-	-	0.0	0.938[b]
	1^1B_2	3.239	3.783	-	-	0.009[b]	0.628[b]
Dichloromethane							
MP2[c]	2^1A_1	1.867		0.237		0.212	0.75
	1^1A_2	2.638		0.390		0.0	0.84
	1^1B_2	2.805		0.395		0.069	0.82
SOS-MP2[c]	2^1A_1	1.325	1.710	0.458	0.513	0.148[b]	0.888[b]
	1^1A_2	2.380	2.747	0.493	0.496	0.000	0.930[b]
	1^1B_2	2.738	3.339	0.501	0.454	0.029[b]	0.869[b]
Exp.[d]	CT band I		1.73				
	CT band II		2.79				

[a] ADC(2) results unless specified differently.
[b] SOS-ADC(2) results.
[c] Gas phase geometry.
[d] Ref.[87]

Table 6. Vertical excitation energies ΔE_{exc} (eV) for the three lowest CT states of the anthracene/TCNE parallel complex using the ADC(2) and SOS-ADC(2) methods, respectively, and the cc-pVTZ' basis. Charge transfer [q(CT)] in units of e and oscillator strengths are also shown.

Geometry	State	ΔE_{exc} (eV)		Solv. Shift (eV)		f[a]	q(CT)[a]
		ADC(2)	SOS-ADC(2)	ADC(2)	SOS-ADC(2)		
Gas phase							
MP2	1^1A_2	1.396		-	-	0.0	0.96
	2^1A_1	2.741		-	-	0.055	0.94
	1^1B_1	3.098		-	-	0.0	0.95
SOS-MP2	1^1A_2	1.513	2.138	-	-	0.0	0.978[b]
	2^1A_1	2.779	3.237	-	-	0.045[b]	0.968[b]
	1^1B_1	3.223	3.849	-	-	0.0	0.027[b]
Dichloromethane							
MP2	1^1A_2	0.958		0.338		0.0	0.96
	2^1A_1	2.318		0.423		0.063	0.94
	1^1B_1	2.681		0.417		0.0	0.95
SOS-MP2	1^1A_2	1.064	1.689	0.449	0.449	0.000	0.977[b]
	2^1A_1	2.339	2.790	0.440	0.447	0.052[b]	0.967[b]
	1^1B_1	2.788	3.608	0.435	0.241	0.020[b]	0.742[b]

[a] ADC(2) results unless specified differently.
[b] SOS-ADC(2) results.

Table 7. SOS-ADC(2) selected bond distances (Å), bond length alternation values (BLA) in Å and charge transfer *q*(CT) in *e* units for the optimized excited states of the TCNE complexes. The results refer to the gas phase without CP correction.

Basis set	Aromat./TCNE[a]	CC(aromat.)[b]	BLA[c]	CC(TCNE)	CN	*q*(CT)
			benzene/TCNE			
cc-pVTZ S_1 (1^1A_2)	3.229	1.409	0.060	1.422	1.179	0.970
cc-pVTZ S_2 (2^1A_1)	3.203	1.409	-0.060	1.422	1.179	0.956
			naphtalene/TCNE			
cc-pVTZ' S_1 (2^1A)	3.420	1.406	0.002	1.412	1.180	0.980
			anthracene/TCNE (perpendicular)			
cc-pVTZ' S_1 (2^1A_1)	3.465	1.406	-0.017	1.422	1.179	0.902

[a] perpendicular distance between TCNE and the aromatic counterpart.
[b] average CC distance in the aromatic system.
[c] See Eqs. (1-3).

Table 8. Adiabatic (minimum to minimum) excitation and vertical fluorescence energies ΔE, using the ADC(2) method.[a]

	ΔE (eV)			
	min.-min.		vert. fluoresc.	
	ADC(2)	SOS-ADC(2)	ADC(2)	SOS-ADC(2)
Benzene/ TCNE[b]		1^1A_2		
Gas phase	2.637	3.235	1.932	2.641
Dichloro-methane		2.472[c]		1.443[d]
		2^1A_1		
Gas phase	2.696	3.256	2.033	2.687
Dichloro-methane		2.407[c]		1.377[d]
Naphthalene/ TCNE[e]		2^1A		
Gas phase	1.646	2.326	1.114	1.832
Dichloro-methane		1.659[c]		0.770[d]
Anthracene/ TCNE (perp.)[e]		2^1A_1		
Gas phase	1.452	1.779	0.919	1.330
Dichloro-methane		0.797[c]		-0.134[d]

[a] Methods for geometries optimization: MP2 in case of ADC(2) excited-state calculation and SOS-MP2 in case of SOS-ADC(2) excited-state calculation
[b] cc-pVTZ basis.
[c] Ground state energy computed with ground-state equilibrated solvent and excited state with excited state solvent equilibration
[d] Excited state solvent equilibration and fast electronic solvent relaxation in transition to the ground state
[e] cc-pVTZ' basis.

Figure Captions

Scheme 1. Top (left) and side (right) views of the complexes TCNE/benzene, TCNE/naphthalene and TCNE/anthracene.

Scheme 2. Bond numbering scheme for the aromatic compounds used in the context of the BLA. See text for more details.

Figure 1 . Isodensity plot of the density difference between the 1^1A_1 ground state and the 1^1A_2 excited state for the TCNE/benzene complex; isodensity values +/-0.0035 $e{\cdot}a_0^{-3}$, blue indicates depletion and red increase of electron density.

Figure 2 . Isodensity plot of the density difference between the 1^1A_1 ground state and the 2^1A_1 excited state for the TCNE/benzene complex; isodensity values +/-0.0035 $e{\cdot}a_0^{-3}$, blue indicates depletion and red increase of electron density.

Figure 3. Isodensity plot of the density difference between the 1^1A ground state and the 2^1A excited state for the TCNE/naphtalene complex; isodensity values +/-0.0021 $e{\cdot}a_0^{-3}$; blue indicates depletion and red increase of electron density.

Figure 4 . Isodensity plot of the density difference between the 1^1A_1 ground state and the 2^1A_1 excited state for the TCNE/anthracene complex; isodensity values +/-0.0011 $e{\cdot}a_0^{-3}$, blue indicates depletion and red increase of electron density.

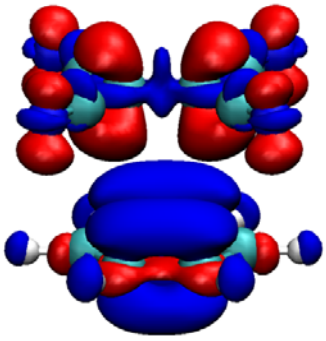

Figure 1. Isodensity plot of the density difference between the 1^1A_1 ground state and the 1^1A_2 excited state for the benzene/TCNE complex; isodensity values +/–0.003535 $e{\cdot}a_0^{-3}$, blue indicates depletion and red increase of electron density.

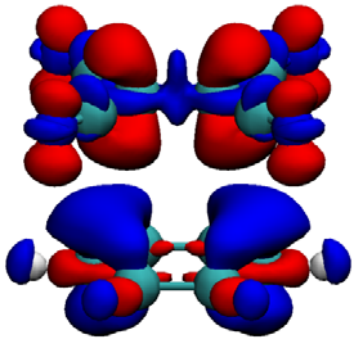

Figure 2. Isodensity plot of the density difference between the 1^1A_1 ground state and the 2^1A_1 excited state for the benzene/TCNE complex; isodensity values +/–0.003535 $e{\cdot}a_0^{-3}$, blue indicates depletion and red increase of electron density.

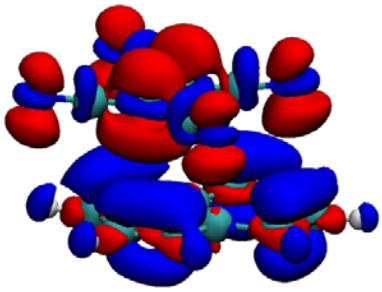

Figure 3. Isodensity plot of the density difference between the 1^1A ground state and the 2^1A excited state for the naphthalene/TCNE complex; isodensity values +/–0.002112 $e{\cdot}a_0^{-3}$; blue indicates depletion and red increase of electron density.

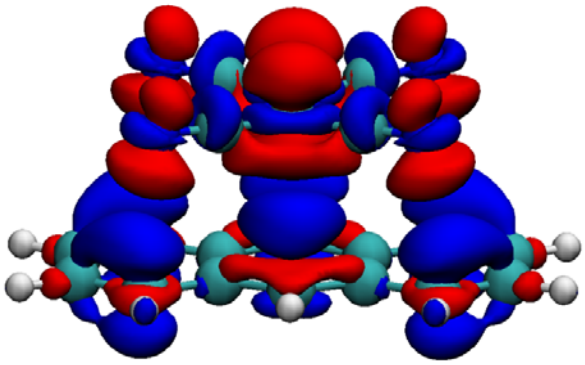

Figure 4. Isodensity plot of the density difference between the 1^1A_1 ground state and the 2^1A_1 excited state for the anthracene/TCNE complex; isodensity values +/–0.00111 $e{\cdot}a_0^{-3}$, blue indicates depletion and red increase of electron density.

References

1. S. Ehrlich, J. Moellmann and S. Grimme, *Acc. Chem. Res.*, 2013, **46**, 916-926.
2. M. S. Liao, Y. Lu, V. D. Parker and S. Scheiner, *J. Phys. Chem. A*, 2003, **107**, 8939-8948.
3. T. Stein, L. Kronik and R. Baer, *J. Am. Chem. Soc.*, 2009, **131**, 2818-2820.
4. A. V. Akimov, A. J. Neukirch and O. V. Prezhdo, *Chem. Rev.*, 2013, **113**, 4496-4565.
5. U. M. Rabie, *J. Mol. Struct.*, 2013, **1034**, 393-403.
6. R. S. Mulliken and W. B. Person, *Molecular Complexes: a Lecture and Reprint Volume*, Wiley-Interscience, New York, 1969.
7. A. C. Benniston and A. Harriman, *Materials Today*, 2008, **11**, 26-34.
8. G. D. Scholes, G. R. Fleming, A. Olaya-Castro and R. van Grondelle, *Nature Chemistry*, 2011, **3**, 763-774.
9. Y. Zhao and W. Liang, *Chem. Soc. Rev.*, 2012, **41**, 1075-1087.
10. J. L. Bredas, J. E. Norton, J. Cornil and V. Coropceanu, *Acc. Chem. Res.*, 2009, **42**, 1691-1699.
11. P. Hobza, *Phys. Chem. Chem. Phys.*, 2008, **10**, 2581-2583.
12. E. C. Lee, D. Kim, P. Jurecka, P. Tarakeshwar, P. Hobza and K. S. Kim, *J. Phys. Chem. A*, 2007, **111**, 3446-3457.
13. K. E. Riley and P. Hobza, *Acc. Chem. Res.*, 2013, **46**, 927-936.
14. D. Kuchenbecker and G. Jansen, *ChemPhysChem*, 2012, **13**, 2769-2776.
15. A. Dreuw, J. L. Weisman and M. Head-Gordon, *J. Chem. Phys.*, 2003, **119**, 2943-2946.
16. C. Adamo and D. Jacquemin, *Chem. Soc. Rev.*, 2013, **42**, 845-856.
17. A. D. Laurent and D. Jacquemin, *Int. J. Quantum Chem.*, 2013, **113**, 2019-2039.
18. H. Iikura, T. Tsuneda, T. Yanai and K. Hirao, *J. Chem. Phys.*, 2001, **115**, 3540-3544.
19. O. A. Vydrov and G. E. Scuseria, *J. Chem. Phys.*, 2006, **125**, 9.
20. A. W. Lange and J. M. Herbert, *J. Am. Chem. Soc.*, 2009, **131**, 3913-3922.
21. L. Kronik, T. Stein, S. Refaely-Abramson and R. Baer, *J. Chem. Theory Comput.*, 2012, **8**, 1515-1531.
22. Q. Wu and T. Van Voorhis, *Phys. Rev. A*, 2005, **72**, 024502.
23. S. R. Yost, L. P. Wang and T. Van Voorhis, *J. Phys. Chem. C*, 2011, **115**, 14431-14436.
24. B. Baumeier, D. Andrienko and M. Rohlfing, *J. Chem. Theory Comput.*, 2012, **8**, 2790-2795.
25. O. Christiansen, H. Koch and P. Jorgensen, *Chem. Phys. Lett.*, 1995, **243**, 409-418.
26. J. Schirmer, *Phys. Rev. A*, 1982, **26**, 2395-2416.
27. V. Lukes, A. Aquino and H. Lischka, *J. Phys. Chem. A*, 2005, **109**, 10232-10238.
28. V. Lukes, A. J. A. Aquino, H. Lischka and H. F. Kauffmann, *J. Phys. Chem. B*, 2007, **111**, 7954-7962.
29. A. N. Panda, F. Plasser, A. J. A. Aquino, I. Burghardt and H. Lischka, *J. Phys. Chem. A*, 2013, **117**, 2181-2189.
30. A. J. A. Aquino, D. Nachtigallova, P. Hobza, D. G. Truhlar, C. Hättig and H. Lischka, *J. Comput. Chem.*, 2011, **32**, 1217-1227.
31. F. Plasser and H. Lischka, *Photochem. Photobiol. Sci.*, 2013, **12**, 1440-1452.
32. C. Hättig, *J. Chem. Phys.*, 2003, **118**, 7751-7761.
33. C. Hättig and F. Weigend, *J. Chem. Phys.*, 2000, **113**, 5154-5161.

34. M. Wormit, D. R. Rehn, P. H. P. Harbach, J. Wenzel, C. M. Krauter, E. Epifanovsky and A. Dreuw, *Mol. Phys.*, 2014, **112**, 774-784.
35. C. Hättig, in *Advances in Quantum Chemistry, Vol 50: A Tribute to Jan Linderberg and Poul Jorgensen*, eds. J. R. Sabin and E. Brandas, Elsevier Academic Press Inc, San Diego, 2005, vol. 50, pp. 37-60.
36. S. Grimme, *J. Chem. Phys.*, 2003, **118**, 9095-9102.
37. Y. S. Jung, R. C. Lochan, A. D. Dutoi and M. Head-Gordon, *J. Chem. Phys.*, 2004, **121**, 9793-9802.
38. A. Hellweg, S. A. Grün and C. Hättig, *Phys. Chem. Chem. Phys.*, 2008, **10**, 4119-4127.
39. N. O. C. Winter and C. Hättig, *J. Chem. Phys.*, 2011, **134**, 184101.
40. C. M. Krauter, M. Pernpointner and A. Dreuw, *J. Chem. Phys.*, 2013, **138**, 044107.
41. N. O. C. Winter, N. K. Graf, S. Leutwyler and C. Hättig, *Phys. Chem. Chem. Phys.*, 2013, **15**, 6623-6630.
42. I. Borges, A. J. A. Aquino, A. Köhn, R. Nieman, W. L. Hase, L. X. Chen and H. Lischka, *J. Am. Chem. Soc.*, 2013, **135**, 18252-18255.
43. J. Tomasi, B. Mennucci and R. Cammi, *Chem. Rev.*, 2005, **105**, 2999-3093.
44. R. Cammi, B. Mennucci and J. Tomasi, *J. Phys. Chem. A*, 2000, **104**, 5631-5637.
45. M. Cossi and V. Barone, *J. Chem. Phys.*, 2001, **115**, 4708-4717.
46. R. Improta, V. Barone, G. Scalmani and M. J. Frisch, *J. Chem. Phys.*, 2006, **125**, 054103.
47. R. Improta, G. Scalmani, M. J. Frisch and V. Barone, *J. Chem. Phys.*, 2007, **127**, 074504.
48. B. Mennucci, C. Cappelli, C. A. Guido, R. Cammi and J. Tomasi, *J. Phys. Chem. A*, 2009, **113**, 3009-3020.
49. A. Klamt and G. Schuurmann, *J. Chem. Soc., Perkin Trans. 2*, 1993, 799-805.
50. A. Klamt, *Wires Comput. Mol. Sci.*, 2011, **1**, 699-709.
51. B. Lunkenheimer and A. Köhn, *J. Chem. Theory Comput.*, 2013, **9**, 977-994.
52. R. E. Merrifield and W. D. Phillips, *J. Am. Chem. Soc.*, 1958, **80**, 2778-2782.
53. I. Hanazaki, *J. Phys. Chem.*, 1972, **76**, 1982-1989.
54. X. Blase and C. Attaccalite, *Appl. Phys. Lett.*, 2011, **99**, 17190.
55. C. Faber, I. Duchemin, T. Deutsch, C. Attaccalite, V. Olevano and X. Blase, *J. Mater. Sci.*, 2012, **47**, 7472-7481.
56. P. Mach, S. Budzak, M. Medved and O. Kysel, *Theor. Chem. Acc.*, 2012, **131**, 14.
57. P. Mach, G. Juhasz and O. Kysel, *Journal of Molecular Modeling*, 2013, **19**, 4639-4650.
58. T. Baruah, M. Olguin and R. R. Zope, *J. Chem. Phys.*, 2012, **137**, 084316.
59. J. M. Garcia-Lastra and K. S. Thygesen, *Phys. Rev. Lett.*, 2011, **106**, 187402.
60. J. C. Stires, E. J. McLaurin and C. P. Kubiak, *Chem. Commun.*, 2005, 3532-3534.
61. M. Kroll, *J. Am. Chem. Soc.*, 1968, **90**, 1097-1105.
62. C. C. Chiu, C. C. Hung, C. L. Chen and P. Y. Cheng, *J. Phys. Chem. B*, 2013, **117**, 9734-9756.
63. C. Møller and M. S. Plesset, *Physical Review*, 1934, **46**, 618-622.
64. F. Weigend, M. Häser, H. Patzelt and R. Ahlrichs, *Chem. Phys. Lett.*, 1998, **294**, 143-152.
65. R. Cammi, B. Mennucci and J. Tomasi, *J. Phys. Chem. A*, 1999, **103**, 9100-9108.
66. K. Sneskov and O. Christiansen, *Wires Comput. Mol. Sci.*, 2012, **2**, 566-584.
67. C. Hättig, D. P. Tew and A. Köhn, *J. Chem. Phys.*, 2010, **132**, 231102.
68. C. J. Cramer, *Essentials of Computational Chemistry: Theories and Models*, John Wiley & Sons, Chichester, 2004.

69. *The CRC Handbook of Chemistry and Physics Internet Version 2005,* http://www.hbcpnetbase.com/, CRC Press, Boca Raton, FL, 2005.
70. T. H. Dunning, *J. Chem. Phys.*, 1989, **90**, 1007-1023.
71. R. A. Kendall, T. H. Dunning and R. J. Harrison, *J. Chem. Phys.*, 1992, **96**, 6796-6806.
72. J. G. Hill, S. Mazumder and K. A. Peterson, *J. Chem. Phys.*, 2010, **132**, 054108.
73. C. Hättig, W. Klopper, A. Köhn and D. P. Tew, *Chem. Rev.*, 2012, **112**, 4-74.
74. S. F. Boys and F. Bernardi, *Mol. Phys.*, 1970, **19**, 553-566.
75. F. Plasser and H. Lischka, *J. Chem. Theory Comput.*, 2012, **8**, 2777-2789.
76. A. E. Reed, R. B. Weinstock and F. Weinhold, *J. Chem. Phys.*, 1985, **83**, 735-746.
77. F. Sterpone and P. J. Rossky, *J. Phys. Chem. B*, 2008, **112**, 4983-4993.
78. R. Ahlrichs, M. Bär, M. Häser, H. Horn and C. Kölmel, *Chem. Phys. Lett.*, 1989, **162**, 165-169.
79. J. Antony and S. Grimme, *J. Phys. Chem. A*, 2007, **111**, 4862-4868.
80. J. G. Hill, J. A. Platts and H. J. Werner, *Phys. Chem. Chem. Phys.*, 2006, **8**, 4072-4078.
81. R. Sedlak, T. Janowski, M. Pitonak, J. Rezac, P. Pulay and P. Hobza, *J. Chem. Theory Comput.*, 2013, **9**, 3364-3374.
82. A. Klamt and V. Jonas, *J. Chem. Phys.*, 1996, **105**, 9972-9981.
83. I. Borges, A. B. Rocha and C. E. Bielschowsky, *Brazilian Journal of Physics*, 2005, **35**, 971-980.
84. F. Plasser, R. Crespo-Otero, M. Pederzoli, J. Pittner, H. Lischka and M. Barbatti, *J. Chem. Theory Comput.*, 2014, **10**, 1395-1405.
85. M. Barbatti, Z. G. Lan, R. Crespo-Otero, J. J. Szymczak, H. Lischka and W. Thiel, *J. Chem. Phys.*, 2012, **137**, 22A503.
86. I. Hanazaki, *J. Phys. Chem.*, 1972, **76**, 1982-&.
87. J. M. Masnovi, E. A. Seddon and J. K. Kochi, *Can. J. Chem.*, 1984, **62**, 2552-2559.